Environmental Science and Pollution Research (2023) 30:101267–101279
https://doi.org/10.1007/s11356-023-29417-5

RESEARCH ARTICLE

Health burden evaluation of industrial parks caused by $PM_{2.5}$ pollution at city scale

Mei Shan[1] · Yanwei Wang[1] · Yuan Wang[1] · Zhi Qiao[1] · Liying Ping[1] · Lien-Chieh Lee[2] · Yun Sun[1] · Zhou Pan[1]

Received: 16 April 2023 / Accepted: 17 August 2023 / Published online: 30 August 2023

Abstract

Industrial park is an important emission sector of $PM_{2.5}$ pollution. Previous studies have provided valuable information on the impact of $PM_{2.5}$ from industrial parks on human health, but relevant studies at city scale are limited. In this study, the health burden of industrial parks was evaluated based on $PM_{2.5}$-related premature deaths and economic contributions. The premature deaths were calculated in terms of a novel research model by integrating the Bayesian maximum entropy (BME) model, weighted concentration-weighted trajectory (WCWT), and integrated exposure-response function (IER). Take Tianjin City for example, it was found that since the main diffusion direction of $PM_{2.5}$ in Tianjin is from south to north, the industrial parks in the south of Tianjin and close to the central city with high population density have high health burden. These industrial parks need to be focused on or even relocated in the future. The research model can provide scientific basis for the health burden evaluation of industrial parks at city scale, so as to help local governments optimize the layout of industrial parks and formulate environmental responsibility management policies for industrial parks.

Keywords Health burden · Industrial parks · Regional transport · $PM_{2.5}$ pollution · Tianjin · City scale

Introduction

Over the past three decades, China's economy has developed rapidly, the process of urbanization has been accelerating, and severe air pollution has followed, especially fine particulate matter ($PM_{2.5}$) pollution (Zhang et al. 2023). High concentrations of $PM_{2.5}$ can directly or indirectly pose a huge threat to public health, causing millions of deaths per year worldwide (4.2 million premature deaths in 2019), with China accounting for the highest proportion of approximately 34% (Huang et al. 2021; Li et al. 2022). Therefore, the Chinese government has formulated a series of prevention and control measures to improve air quality since 2013 (Xu et al. 2023), and the first interim and guideline targets of the WHO have been achieved in 2020. Despite the substantial reduction, $PM_{2.5}$ still exceeded the limit of WHO $PM_{2.5}$ guideline of 10 mg/m^3 and heavy pollution episodes occasionally happened.

Spatial and temporal variations in $PM_{2.5}$ pollutants are highly dependent on regional transport and local pollutants emissions (Chen et al. 2020). Therefore, tracking the potential sources of $PM_{2.5}$ is significant for reducing pollutant concentration. At the same time, $PM_{2.5}$ atmospheric transport can significantly influence the distribution of health effects, which have been indicated by some studies at different spatial scales. For example, non-local emissions of atmospheric pollution transport contributed 50–73% of the $PM_{2.5}$-related premature deaths in the Beijing-Tianjin-Hebei region in 2017 (Jiang et al. 2021); non-local transport impact accounted for approximately 30% in all regions of China, and further combined with economic data, the regions and sectors with the highest health burden ($PM_{2.5}$ related premature deaths per unit output or consumption) included the manufacturing and household sectors in North and Northeast China and transportation, agriculture, and electricity in Central China (Ping et al. 2023). Pollution and health analysis based on pollutant transport provides a crucial scientific basis for carrying out air pollution control cooperation and tracking pollution responsibilities.

Responsible Editor: Lotfi Aleya

✉ Yuan Wang
wyuan@tju.edu.cn

[1] School of Environmental Science and Engineering, Tianjin University, Tianjin 300350, China

[2] School of Environmental Science and Engineering, Hubei Polytechnic University, Huangshi 435003, Hubei, China

Furthermore, the pollution emission from industrial production is the essential cause of Chinese environmental issues, and production is mainly governed and managed by local industrial parks (Xu et al. (2017a)). The development of Chinese industrial parks started with the Shekou Industrial Zone in 1979 (Wang and Bradbury 1986). After more than 40-year development, China has developed over 6000 industrial parks, which form a complete and diverse industrial system and contribute to over 50% of the gross industrial output value (Lyu et al. 2022). While increasing the output value, industrial production also results in serious air pollution in industrial parks and surrounding areas in China, which poses a threat to the living environment, health, and even life of human beings (Han et al. (2019a)). Many studies have explored the concentrations and health impacts of $PM_{2.5}$ pollution, or its precursor NOx and VOCs in industrial areas. For example, Chen et al. (2021) and Zheng et al. (2020) used the United States Environmental Protection Agency (USEPA) health risk method to assess cancer and non-cancer health risks of volatile organic compounds (VOCs) at an industrial park. Zhang et al. (2021) selected the average daily dose (ADD) to express a spatial exposure level of NOx for a typical industrial park to identify NOx health risk zones. Based on the entropy weight method and traditional USEPA method. Sun et al. (2021) assessed the health risks of $PM_{2.5}$ heavy metal in an industrial park in northeast China.

The efficient control of $PM_{2.5}$ pollution in industrial parks requires tracking pollution sources and analyzing their health burden (Huang et al. (2020a); Ping et al. 2023). Previous studies have provided valuable information for the health management of the population in industrial parks. However, most studies focused on a particular industrial park. There are few studies on the health burden research of $PM_{2.5}$ pollution on multiple industrial parks at the city scale, and few combining premature deaths with economic data to discuss the health burden of industrial parks based on the effect of pollution transport. At present, a city in China generally has more than one industrial park. These parks are the largest contributors to city $PM_{2.5}$ pollution emissions (Wu et al. 2016; Zheng et al. 2020). The emissions and uncontrolled transport from these industrial parks pose significant potential health impacts to city residents. Therefore, how to evaluate and lay out these industrial parks and develop more effective control strategies are the thorny problems in city atmospheric environment management in China. The research and development in this field also are limited due to the lack of publicly released detailed monitoring data on China's industrial parks.

With the above considerations, in order to evaluate industrial parks from the perspective of the health effects of $PM_{2.5}$ pollution, this paper tries to establish a new research model based on generally available data. We introduce the Bayesian maximum entropy (BME) model with retrospective analysis of $PM_{2.5}$ data derived from NASA Global Modeling and Assimilation Office into a backward trajectory model and exposure-response function (IER) to evaluate the $PM_{2.5}$ health burden of industrial parks. The BME is a geostatistical method for simulating spatial/temporal data based on epistemic, which can account for missing data by utilizing a nonlinear formulation of the probability density function (PDF) at each spatiotemporal point (Chen et al. 2018; Christakos 1990). The weighted concentration-weighted trajectory (WCWT) analysis can semi-quantify the contribution of different source areas for $PM_{2.5}$ pollution (Wang et al. 2006, 2009; Lin et al. 2022), and the integrated exposure-response function (IER) can be applied to assess the health burden resulting from $PM_{2.5}$ exposure (Cao et al. 2022). As a consequence, $PM_{2.5}$ concentrations evaluated by BME can be coupled with the backward trajectory method and IER to geographically and rapidly identify air masses that contain a high concentration detected at the receptor site, and calculate the health impacts of $PM_{2.5}$ exposure. The above hybrid method is defined as the combined BME-WCWT-IER method.

Take Tianjin, one of the most polluted cities for $PM_{2.5}$ in China, for example, we applied the above model to evaluate the premature deaths that may be caused by $PM_{2.5}$ in 147 industrial parks in Tianjin. Combined with the economic contribution of each industrial park, we can assess the health burden of each park and put forward policy recommendations according to different levels. This research model can also be extended to other industrial cities similar to Tianjin, providing new ideas and scientific quantitative tools for city-level atmospheric environment quality management.

Data and methods

Study area

Tianjin is a coastal megacity in the Jing-Jin-Ji Metropolitan Region, adjacent to the Bohai Sea (Fig. 1). It is influenced by a warm continental monsoon climate. The average temperature is 26~27 °C in summer and −3~5 °C in winter. Tianjin has a population of more than 13 million, and a GDP of over RMB 1500 billion in 2021. In recent years, $PM_{2.5}$ pollution has frequently occurred in Tianjin due to the growing population, rapid industrialization, heavy traffic, and climatic conditions. Of which, the pollution emission from industrial production is considered to be predominant in Tianjin, especially from industrial parks (Wang et al. 2016). The basic information on industrial parks in each district of Tianjin is shown in Table 1.

Data collection and processing

The monitoring data of $PM_{2.5}$ concentrations were obtained from the China National Environmental Monitoring Centre (CNEMC) for the period March 2017 to February 2021 (Fig. S1 and Table 2). Meteorological data were originated from the National Centers for Environmental Prediction (NCEP) reanalysis data, and downloaded from the Global

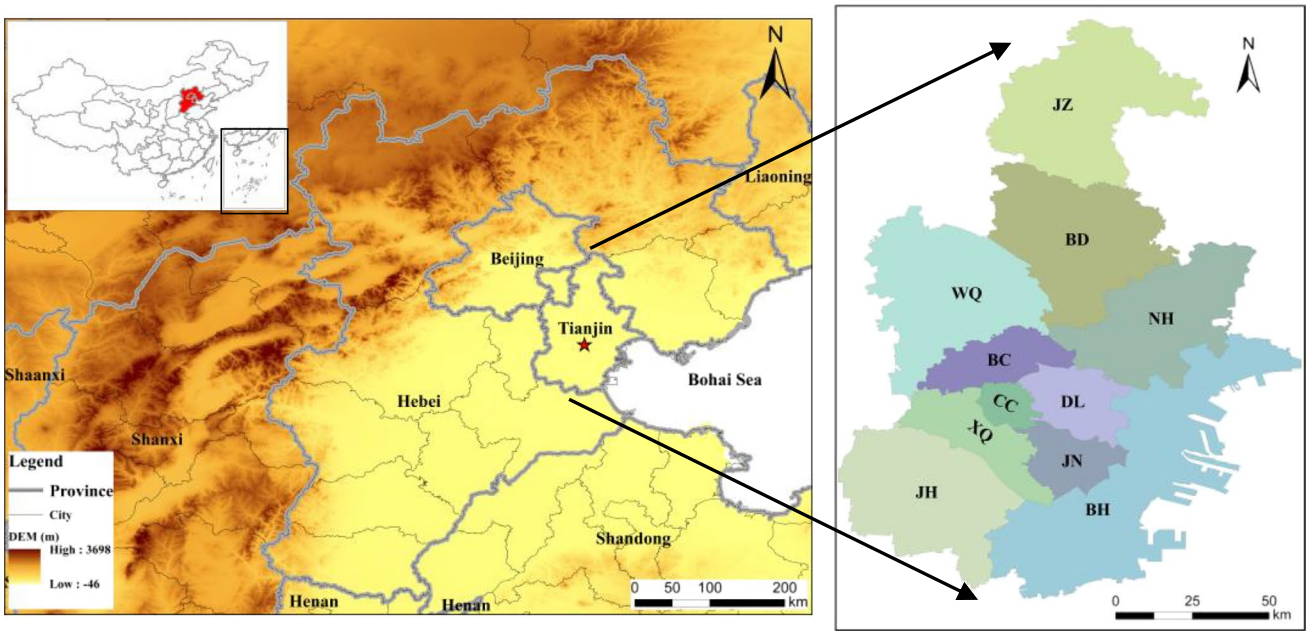

Fig. 1 Location of Tianjin and surrounding provinces. The abbreviations of districts in Tianjin are DL, Dongli; XQ, Xiqing; CC, central city; JN, Jinnan; BC, Beichen; WQ, Wuqing; BD, Baodi; BH, Binhai New Area; NH, Ninghe; JH, Jinghai; JZ, Jizhou

Table 1 Basic information on industrial parks in Tianjin

Districts	Southern Tianjin							Northern Tianjin				
	BH	DL	JH	XQ	BC	JN	Total	WQ	BD	NH	JZ	Total
Number of industrial parks	24	7	9	15	21	14	90	30	18	6	3	57
Area percentage of industrial parks	36%	15%	11%	7%	6%	4%	79%	9%	6%	4%	2%	21%

Table 2 Data source and description

Data type	Time	Data source
$PM_{2.5}$ monitoring data	2017.03–2021.02	China National Environmental Monitoring Centre (http://www.cnemc.cn/)
Meteorological data GDAS1	2017.03–2021.02	National Centers for Environmental Prediction (ftp:// arlftp. arlhq. noaa. gov/ pub/ archi ves/ gdas1)
Meteorological observed data	2017.03–2021.02	National Climatic Data Center (ftp://ftp.ncdc.noaa.gov/pub/data/noaa/isd-lite/)
MERRA2 data	2017.03–2021.02	NASA Global Modeling and Assimilation Office (https://disc.gsfc.nasa.gov/datasets/M2T1NXAER_5.12.4/summary?keywords=M2T1NXAER)
Population data	2017–2020	Tianjin Statistical Yearbook (https://stats.tj.gov.cn/tjsj_52032/tjnj/)
Emission data	2017	Multi-resolution Emission Inventory for China (MEIC) (http://www.meicmodel.org/)
Economic output	2017–2020	Unreleased government documents

Data Assimilation System (GDAS), and meteorological observed data in Tianjin station (39.100 °N, 117.167 °E) from the National Climatic Data Center. Moreover, the annual data in this paper are from March to February of the next year. Based on the climate in the Northern Hemisphere, the seasonal data are from March to May for spring, June to August for summer, September to November for autumn, and December to February of the following year for winter.

The ground-level monitoring can realize accurate $PM_{2.5}$ measurements, but it has limited spatial resolution and coverage (Fig. S1 (a)). The Modern Era Retrospective Analysis for Research and Applications, version 2 (MERRA-2), can compensate for the lack of an air pollution monitoring network, with 72 vertical hybrid-eta levels from the surface to 0.01 hPa, a temporal resolution of 1 h, and a spatial resolution of 0.5° × 0.625° (latitude × longitude) (Fig. S1 (b)). The MERRA-2 was obtained from the NASA Global Modeling and Assimilation Office (GMAO) in 2017 (Randles et al. 2017). MERRA-2 is based on the Goddard Earth Observing System version 5 (GEOS-5) model and analysis system, which offers not only a reanalysis in the field of meteorology but also several parallel re-analyses of the Earth system's other components, such as the ocean, land, and atmospheric component. Of particular interests for this paper are the MERRA-2 analyzed aerosol species. The MERRA-2 total $PM_{2.5}$ concentrations can be defined as follows:

$$PM_{2.5}^{MERRA2} = \left[Dust_{2.5}\right] + \left[SS_{2.5}\right] + [BC] + 1.6 \times [OC] + 1.375 \times \left[SO_4\right] \quad (1)$$

where $[Dust_{2.5}]$, $[BC]$, $[SS_{2.5}]$, $[OC]$, and $[SO_4]$ represent the concentrations of dust, *BC*, *SS*, *OC*, and sulfate particulates, respectively, with diameters less than or equal to 2.5 μm. Detailed information on factors of species can be seen in previous related papers (Song et al. 2018; Zhang et al. 2013).

Methods

In this study, the integration of data and methods from multiple sources and disciplines was required, as shown in Fig. S2. Firstly, we applied BME to accurately evaluate the temporal and spatial distribution of $PM_{2.5}$ concentrations by fusing monitoring data and MERRA2 data. According to the $PM_{2.5}$ estimations, we then used the WCWT to analyze the contribution of inter-district transport effects for atmospheric particles and used IER to calculate the health impact of each district. Next, the health impact of Tianjin caused by each district was obtained based on the above two results. Considering the industrial source emission and the industrial park area ratio, we subsequently calculated the health impacts of each industrial park. Finally, the typical industrial parks' health burden was classified in terms of health impact and economic output.

The combined BME-WCWT-IER method

BME analysis According to MATLAB R2012a and BMElib 2.0b, the BME analysis is performed using SEKS-GUI v1.0.3. The BME framework is based on a spatiotemporal random field (RF) representation of $PM_{2.5}$ $R(p)$, where $p = (s,t)$ represents the spatiotemporal coordinate, consisting of a set of specific spatiotemporal data points p_d and the estimation point p_k. s denotes the spatial location, and t denotes time. The process of BME analysis can be summarized in three stages (Reyes and Serre 2014; Shan et al. 2021; Xu et al. (2017b)). Prior stage, covariance and variance of the $PM_{2.5}$ concentrations are estimated in terms of hard data χ_{hard} and soft data χ_{soft}. In our study, the $PM_{2.5}$ concentrations measured were considered hard data and the $PM_{2.5}^{MERRA2}$ from MERRA2 were considered soft data. Then, based on the covariance function of $PM_{2.5}$ concentrations and mean trend function, the prior probability density function (PDF) f_G of all points is estimated. f_G is defined by Eq. (2).

$$f_G\left(\chi_{map}\right) = \exp\left(\mu 0 + \mu^T g\right) \quad (2)$$

where random variables' vector $\chi_{map} = [\chi_{data}, \chi_k]$, $\chi_{data} = [\chi_{hard}, \chi_{soft}]$ represents the hard and soft data values at mapping points. χ_k indicates the predicted value at the estimated point. μ_0 represents a constant term reflecting the normalized constraints, μ is the coefficient vector related to g, and g is the function vector of G with the largest amount of information.

Meta-prior stage, site-specific knowledge (S), consisting of hard and soft data, will be expressed in a proper form. Posterior stage, the posterior probability density function f_K is estimated by considering S and $f_{G,}$ which are obtained on the basis of operational Bayesian conditionalization. According to f_k, the predicted mean $\hat{\chi}_{k,mean}$ of the estimated points can be estimated, and the horizontal resolution was 1 km×1 km. $\hat{\chi}_{k,mean}$ shown by Eq. (3).

$$\hat{\chi}_{k,mean} = \int \chi_k f_{k(\chi_k)} d_{\chi_k} \quad (3)$$

The 10-fold cross-validation (CV) was used to evaluate BME model performance. Tenfold CV randomly divides the data into 10 subsets of equal size from all sites. Each subset is then utilized in turn to validate the model trained by the remaining 9 subsets. R^2 and root mean squared error (RMSE) were applied as fitting measures of the final model. RMSE is a metric representing the differences between the predicted values and the observed values.

WCWT model Backward air mass trajectories originated from the Hybrid Single Particle Lagrangian Integrated Trajectory (HYSPLIT) model, which was applied to recognize transport pathways (Huang et al. (2020b)). In our

paper, the accuracy of meteorological data GDAS1 input to the HYSPLIT model was verified firstly (Fig. S3). Twenty-four-hour backward trajectories arriving at the centers of 11 districts in Tianjin were then calculated every 1 h at 500 m above the ground level (Table S1). The WCWT analyses (Wang et al. 2006, 2009; Wang et al. 2022) are conducted to assess the weight concentration of the airflow trajectory in potential source areas based on MeteoInfo Software with the TrajStat Plugin, which can reflect the pollution degree of different trajectories. The method divided the research area into small equal grids, and the area of each grid was 0.09°×0.09°. We used the Spatial Join tool (ArcGIS 10.2) to partition the BME predictions to obtain the $PM_{2.5}$ concentrations of each district, which was one of the input data for the WCWT analysis. The WCWT value for the *ij*th cell is expressed as follows:

$$WCWT_{ij} = \left(\sum_{l=1}^{N}\left(C_l \times \alpha_{ijl}\right)/\sum_{k=1}^{N}\alpha_{ijl}\right) \times W(ij) \tag{4}$$

where N is the total number of trajectories passing through the grid ij, C_l is the pollutant concentration carried by trajectory h in the grid ij and estimated by BME according to Eq. (3), α_{ijl} is the residence time of trajectory l in grid ij, and the weighted function W_{ij} is applied to decrease the uncertainty in the calculation of the trajectory weight concentration (Tang et al. 2017). The descriptions of W_{ij} are provided in Table S2.

The WCWT only reflects the potential transport contribution of the source region, but cannot support the division of pollution responsibility. Therefore, to further analyze the potential input-output balance, we defined the potential source and receptor of districts according to the concentration-weighted trajectory of net pollution ($WCWT_{net}$). $WCWT_{net}$ is estimated as follows:

$$WCWT_{net}^{rs} = WCWT^{sr} - WCWT^{rs} \tag{5}$$

where $WCWT_{net}^{rs}$ is the net potential contribution of air pollution in district s relative to r. When $WCWT_{net}^{rs} > 0$, district s is a potential source district; conversely, district s is a potential receptor district. $WCWT^{sr}$ is the potential contribution of air pollution in district r originating from emission in region s.

IER model The integrated exposure-response function (IER) is currently a popular method for assessing disease deaths due to $PM_{2.5}$ pollution, developed by Burnett et al. (2014). The model mainly includes five pollution-related diseases: stroke, ischemic heart disease (IHD), lung cancer (LC), chronic obstructive pulmonary disease (COPD), and acute respiratory lung infection (ALRI). There is a relative lack of research data on ALRI disease in China, mainly for children under 5 years old, so we only study the first four diseases that have received widespread attention. The specific relative risk (RR) is expressed as follows:

$$RR(C) = \begin{cases} 1 + \alpha\left(1 - \exp\left(-\beta\left(C - C_0\right)^{\gamma}\right)\right), C > C_0 \\ 1 \qquad\qquad\qquad\qquad , else \end{cases} \tag{6}$$

where α, β, and γ are nonlinear parameters used to depict the different shapes of the RR curve among different diseases (Cao et al. 2022); C_0 is the threshold value; C indicates the $PM_{2.5}$ concentration evaluated by the BME model according to Eq. (3). The specific value of each parameter is shown in Table S3 (Lee et al. 2015). In addition, the mortality burden is evaluated by the health impact function (Eq. (7)).

$$M = B \times P \times (1 - 1/RR) \tag{7}$$

where M is the premature mortality depending on specific diseases owing to $PM_{2.5}$; B is the baseline mortality rate (Table S3); P is the population exposed to $PM_{2.5}$. The population data in 2020 are obtained from the Tianjin Statistical Yearbook (Tianjin Statistical Yearbook 2021).

The combined BME-WCWT-IER Based on the BME-WCWT-IER models, we can obtain the health impact of each district, which is calculated by:

$$H_{WCWT}(r) = \sum_{s=1}^{n}\left(M^s \times WCWT^{rs}/WCWT_{in}^{s}\right) \tag{8}$$

where $H_{WCWT}(r)$ expresses the number of premature deaths in Tianjin caused by district r, n is the total number of districts in Tianjin, M^s is the number of premature deaths in district s, $WCWT_{in}^{s}$ is the total potential transport effect of all districts in Tianjin on the district s, and $\frac{WCWT^{rs}}{WCWT_{in}^{s}}$ indicates the percentage of the potential transport effect of the district r on the district s. M and $WCWT$ values are calculated based on BME.

The health burden evaluation of industrial parks

According to the health impact of each district estimated by the BME-WCWT-IER methods and the economic output of each industrial park, the health burden of industrial parks is calculated. Firstly, we estimated the health impact of each district caused by industrial pollution, which is calculated by taking the emission ratio of industrial sources to anthropogenic sources as the weight, based on MEIC. Then, the health impact of each industrial park is calculated using the area of the industrial park as the weight. Finally, based on the above considerations and each industrial park's economic output, each park's health burden is expressed by premature deaths per unit output.

Results and discussions

Validation of $PM_{2.5}$ concentration simulated by BME model

Due to the lack of high-resolution $PM_{2.5}$ concentration monitoring data, we employed the BME model using MERRA2 data and ground monitoring data to simulate $PM_{2.5}$ concentrations in Tianjin from 2017 to 2020. The validation scatterplots for the BME model are shown in Fig. S4. The BME model has good performance characteristics, with an R^2 of 0.81 and RMSE of 10.2 μg m^{-3}. There have been many studies comparing the simulation results of BME with other models, proving that BME was able to improve the simulation accuracy of $PM_{2.5}$ concentrations (Table 3). Compared to the performance of these studies (R^2: 0.71–0.88, RMSE: 11.39–18.81 μg m^{-3}), our BME model with MERRA2 as soft data performs moderately well. The BME model is sensitive to the quality of soft data. The comparison results show that the simulation accuracy of $PM_{2.5}$ concentrations can be improved to some extent by using MERRA2 as soft data.

Figure 2 represents the spatial and temporal variations of $PM_{2.5}$ concentrations simulated by the BME model in Tianjin with a 1 km resolution. The spatial gradients of $PM_{2.5}$ concentrations showed similar during the four seasons, and the overall $PM_{2.5}$ concentration trend in the study region was low in the north and high in the south. The temporal $PM_{2.5}$ concentrations showed a clear seasonal variation with the lowest in summer and the highest levels in winter in the study region. This variation is consistent with the official result released by Tianjin Ecological Environment Bureau (Figs. S5–S6). This also shows that the $PM_{2.5}$ concentration simulated by BME is relatively reliable.

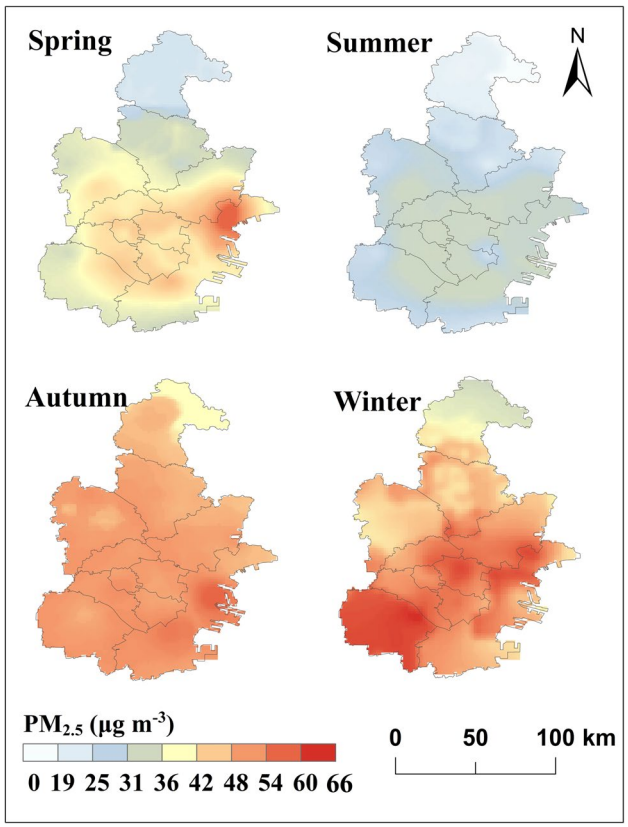

Fig. 2 The simulation maps of $PM_{2.5}$ concentrations in Tianjin

Inter-district transport and health impact analysis of $PM_{2.5}$ within city

The 147 industrial parks in Tianjin are distributed in 11 districts, and the $PM_{2.5}$ pollution transport patterns and health impacts of each district are different. In order to

Table 3 Typical $PM_{2.5}$ estimation models and verification results

References	Research region	Data	Models	R^2	RMSE (μg m^{-3})
Beckerman et al. (2013)	Contiguous United States	Monitoring, land use, traffic, and remotely sensed data	LUR	0.16	/
			LUR-BME	0.79	/
Cleland et al. (2020)	California	Monitoring station data, community multiscale air quality model data, and satellite-derived estimates	CMAQ	0.46	/
			BME	0.71	/
Xiao et al. (2018)	Mainland China	Satellite-derived aerosol optical depth (AOD), topography data, meteorological data, and pollutant emission	GWR	0.75	14.87
			GWR-BME	0.88	11.39
Xiong et al. (2021)	Anhui Province, China	Himawari-8 AOD, meteorological data, population density, the normalized difference vegetation index, and gross domestic product	GAM	0.44	18.81
			GAM-BME	0.81	12.45

Note: the abbreviations of community multiscale air quality, geographically weighted regression, and generalized additive model are CMAQ, GWR, and GAM; LUR-BME represents the hybrid model of LUR and BME, others are similar

evaluate each industrial park, we first analyzed the impact of air pollution transport and its health in each district. To understand the pollution transport among different districts inside the city, it is necessary to explore the inter-district net transport contribution of $PM_{2.5}$ pollution according to Eq. (5), and the results are expressed in Fig. 3. The positive total net WCWT values in JH, JN, BH, and DL Districts located in the south of Tianjin showed that the $PM_{2.5}$ outflows of these districts greatly exceeded the inflows. Therefore, these areas are the "source" of $PM_{2.5}$ from the perspective of a city as a whole. Alternatively, JZ, WQ, and BD Districts located in the north of Tianjin with negative total net WCWT values acted as "receptors" of $PM_{2.5}$. The above results indicated that the main diffusion direction of $PM_{2.5}$ within Tianjin is from south to north in all seasons due to more intensive industrial parks and population in the south. Compared with the industrial parks in northern districts, there are more industrial parks in southern districts, accounting for a larger proportion (79%) of the area of all industrial parks (Table 1). The population density in the southern districts is about 7 times that of the northern districts (Tianjin Statistical Yearbook 2021). Previous studies also proved that the major potential sources that were likely contributors of $PM_{2.5}$ were situated in the southwest of Tianjin. For example, the southwestern airflow in Tianjin corresponded to higher $PM_{2.5}$ concentrations in all seasons (Wang et al. 2022); the southerly pathway represented the major transport pathway of $PM_{2.5}$ for all seasons (Hao et al. 2019). This shows that the transport direction inside and outside Tianjin is generally consistent.

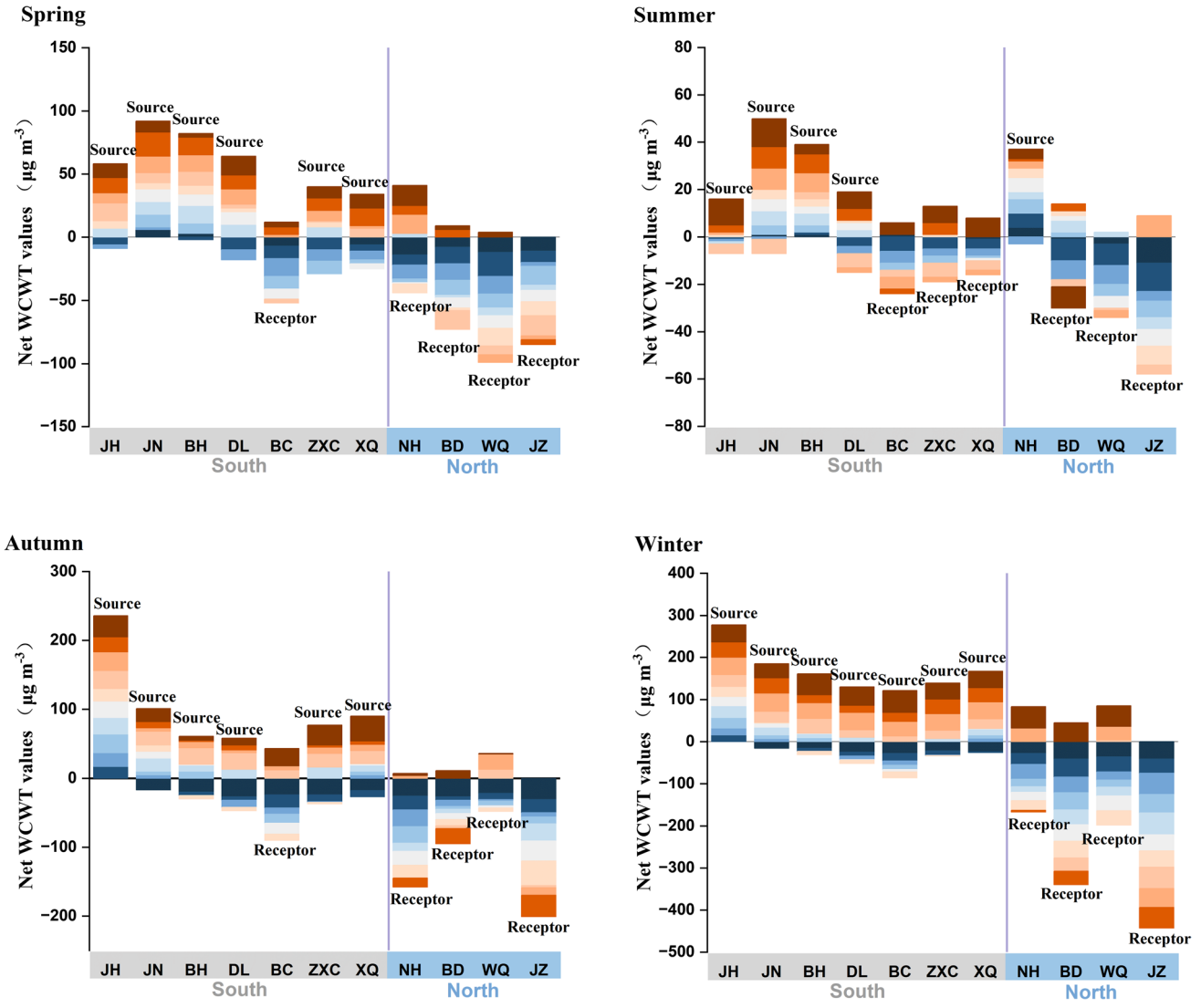

Fig. 3 Net transport contribution of $PM_{2.5}$ pollution within Tianjin. Negative values express the potential receptors; positive values express the potential sources

Moreover, the net WCWT values are significantly higher in winter than in other seasons. Owing to the large amount of air pollutants generated by the heat supply, there is a high potential for $PM_{2.5}$ pollution transport within Tianjin in winter. At the same time, the high-frequency calm and stable weather due to temperature inversion and terrain barrier in winter will limit environmental capacity and cause very unfavorable diffusion conditions (Wu et al. 2021). There are no seasonal differences in source and receptor roles in 64% of the districts. Only a few districts are different, probably due to the smaller area of the district and the consequent smaller local emissions, while the impact of out-of-district is significant.

Moreover, the $PM_{2.5}$-related premature deaths of each district were estimated based on Eq. (7) (Fig. S7). The results showed that the 4-year average number of deaths in Tianjin is 4310 deaths (95% CI: 2739; 5641) during 2017–2020. Previous studies have conducted similar simulations using the IER model: the numbers of deaths attributed to $PM_{2.5}$ in Tianjin were 19,100 (95% CI: 14,500; 21,800) and 15,900 deaths (95% CI: 11,600; 18,600) in 2013 and 2017, respectively (Ding et al. 2019); in Tianjin, the $PM_{2.5}$-attributable premature deaths in 2020 ranged from 20 to 100 deaths per 100 km^2 (Li et al. 2022). The premature deaths per 100 km^2 in our case were 37 deaths per 100 km^2 (23–48 deaths per 100 km^2). Obviously, the number of premature deaths estimated in this study was lower than that of the aforementioned studies, especially that in Ding et al. (2019), which may be related to the low concentration simulated by BME, as the relatively low concentration of input data MERRA2. However, the main reason is the improvement of ambient air quality. In recent years, the control of $PM_{2.5}$ had made substantial progress after the Chinese government implemented the Clean Air Action Plan during 2018–2020 (Xu et al. 2023). Moreover, to reduce the impact of COVID-19 (coronavirus disease), China adopted lockdown measures, which could be a benefit with levels of $PM_{2.5}$ pollutants falling (He et al. 2020).

The inter-district health impacts associated with $PM_{2.5}$ were further estimated based on Eq. (8), which are shown in Fig. 4. From the source's perspective, there is little variation in health impacts across districts ranging from 95 to approximately 179 $PM_{2.5}$-related premature deaths (variance = 22) (Fig. 4 (a)). From the receptor's perspective, it is worth noting that the CC District, with 493 premature deaths related to $PM_{2.5}$, has the highest health impact due to its largest population than other districts (Fig. 4 (b)). If we consider the net number of premature, except for the CC, the net $PM_{2.5}$-related premature death is 340; there is little difference in other districts, between −43 and approximately 98 (Fig. 4 (c)). Therefore, compared with the "source" and "receptor" role with significant differences between south and north in Fig. 3, considering the net premature death among regions related to $PM_{2.5}$, as shown in Fig. 4, the health impact difference of $PM_{2.5}$ between north and south is not significant. This is mainly reflected in the impact of population density. Based on the above research, the environmental health responsibility of industrial parks in each district is not necessarily consistent with the emission and concentration of $PM_{2.5}$ in the area where they are located, but also relates to the population density in the affected area. On this basis, the health impact of industrial parks can be more carefully assessed.

Health burden evaluation of industrial parks and policy implications

According to the results of inter-district transport analysis of $PM_{2.5}$ (Eq. (4) and (5)) and the health impact of districts (Eq. (8)), the $PM_{2.5}$-related premature deaths were calculated for each industrial park. Then, the health burden of 147 industrial parks in Tianjin was evaluated based on their health impact from $PM_{2.5}$ pollution and industrial output (Fig. 5).

The industrial parks with high health burden account for 24% of all industrial parks area (Fig. 5). These industrial parks are mainly concentrated around the CC. The leading industry in these parks features relatively high air pollution, including ferrous metal smelting, cement manufacturing, and rubber and plastic production. According to the "Inter-district transport and health impact analysis of PM2.5 within city" section, the direction of pollution transport within Tianjin is from south to north. Consequently, large quantities of $PM_{2.5}$ emitted by these industrial parks transport northward, especially to the nearest in the north densely populated CC, causing more serious health impacts. As a result, immediate action needs to be taken to alter this industrial layout and reduce $PM_{2.5}$ pollution emissions. On the one hand, we suggest phasing out or relocating small industrial parks with significant air pollution away from these districts around the CC. The relocation site of these industrial parks may consider potential receptor districts, while also taking into account other factors such as the climatic and geographical conditions of the site. On the other hand, for industrial parks located in the south of Tianjin and occupying a large area, it is difficult to shut down or relocate all of them. Therefore, air pollution reduction technology is particularly important for these industrial parks. It is worth noting that the two small industrial parks in JZ District have a high health burden, although air quality in this district is relatively good in Tianjin. The two parks are dominated by light industries, such as food and beverage manufacturing. The economic activities of light industries involve lower energy consumption, lower proportions of processed or semi-processed materials, and also much lower air pollution impacts. Therefore, it is suggested that such industrial parks mainly improve the added value of their light industry, and pay attention not to increase additional air pollution emissions.

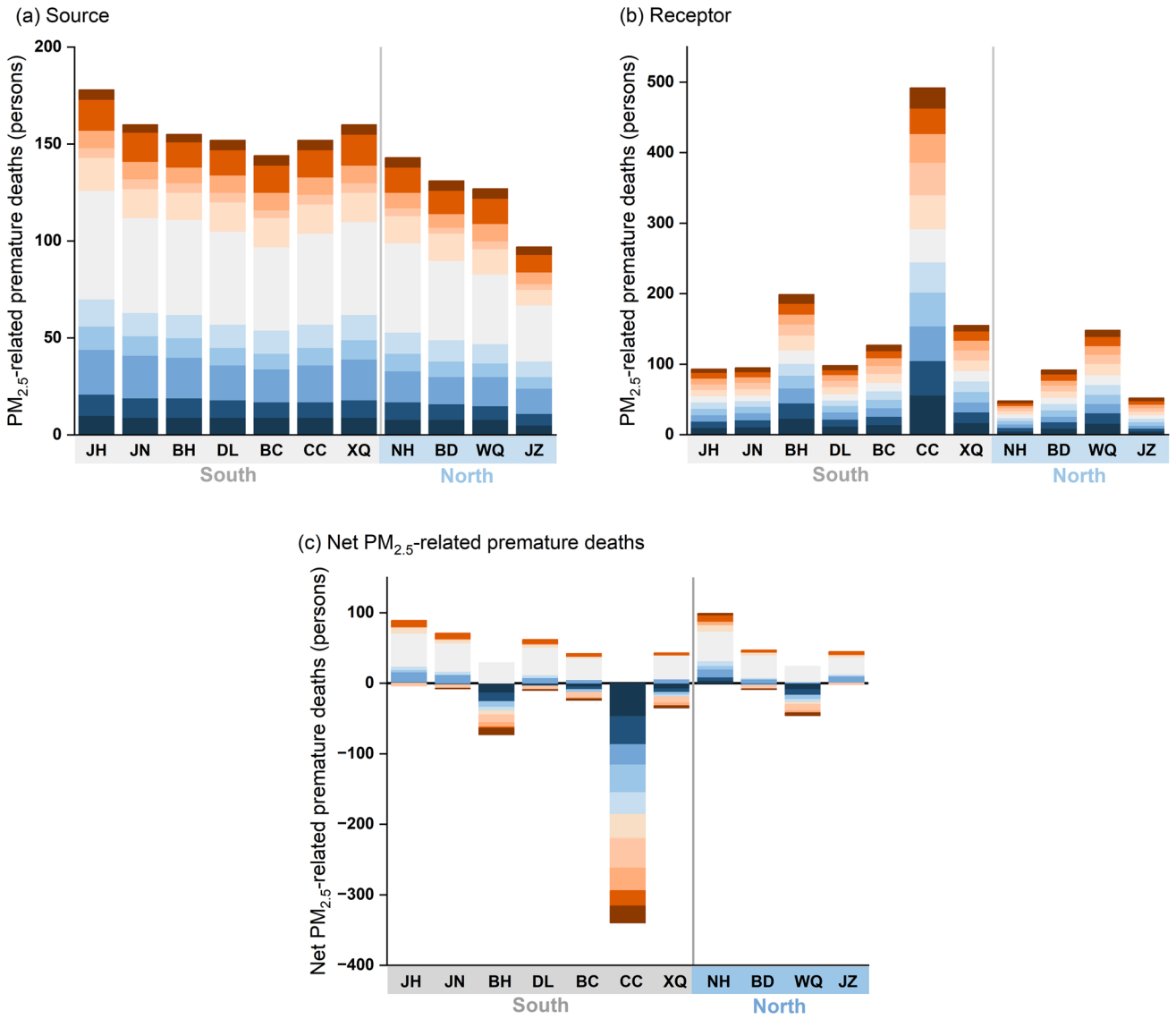

Fig. 4 $PM_{2.5}$-related premature deaths from the perspective of **a** source and **b** receptor, and **c** net $PM_{2.5}$-related premature deaths in Tianjin

The area proportion of industrial parks with low health burden is the largest (51%) among the three classification results of industrial parks (Fig. 5). These industrial parks are concentrated in the coastal region of Tianjin. They have a relatively low health impact and relatively high industrial output because their leading industries are focused on science and technology promotion and application services, computer, communications, and other electronic equipment manufacturing. At the same time, the atmospheric diffusion conditions of these industrial parks along the coast are also relatively superior (Han et al. (2019b)). The effect of the sea and land breezes on the diffusion of $PM_{2.5}$ pollution is significant. Thus, these industrial parks should be the key development direction in the future. Furthermore, the remaining industrial parks with health burden varying from 1.67 to approximately 3.33 deaths/billion yuan account for 25% of all industrial parks area. These industrial parks are concentrated in the BD, WQ, and JN Districts, and contain more diversified industries. This type of industrial park should adopt different management and pollution prevention measures according to each park's leading industry, land area, and geographical location, but can generally follow the principle of increasing economic output while maintaining or reducing $PM_{2.5}$ pollution emissions.

Uncertainty and limitation analysis

This study has several uncertainties and limitations derived from the BME, WCWT, and IER models.

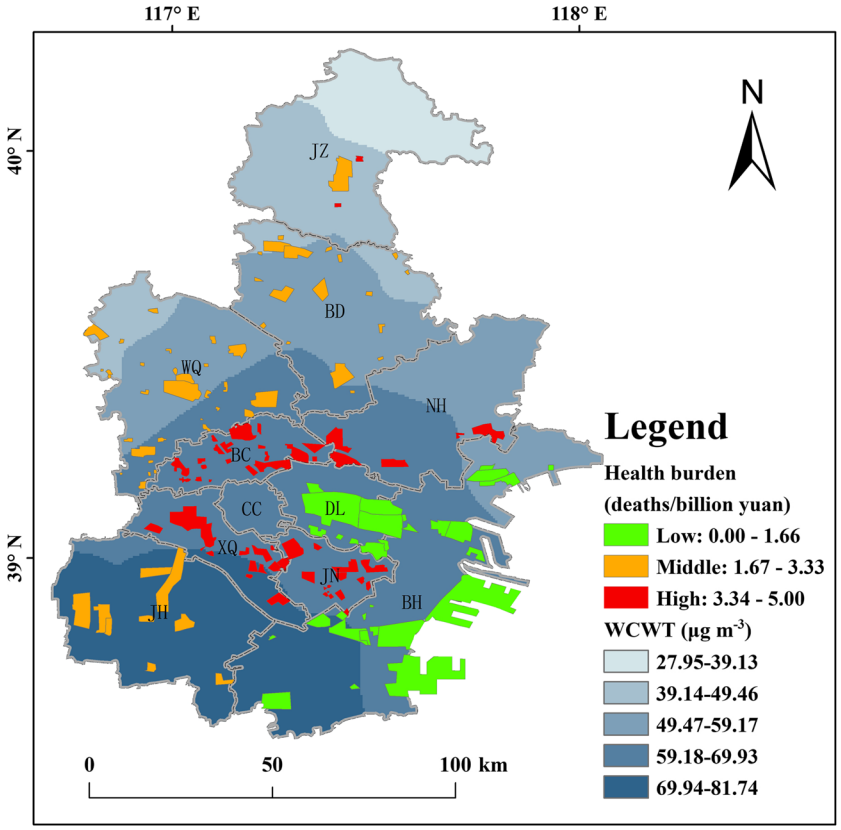

Fig. 5 Health burden evaluation of industrial parks

Firstly, BME as a modern geographical statistical model BME; the significant uncertainty of this model is derived from the fact that it requires assumptions about the prior distribution of parameters, which will affect the final results (Christakos 1990; Xiao et al. 2018). Furthermore, the performance of the BME model largely depends on the amount of observed data and its distribution density (Cleland et al. 2020). The coverage of air quality ground monitoring sites is limited. In this study, we applied the BME model combined with MERRA2 data to compensate for the shortcomings of ground monitoring data, but the $PM_{2.5}$ concentration calculated by MERRA2 is relatively low because the nitrate particles predominantly emitted by human activities are not included (Song et al. 2018). Therefore, the simulated $PM_{2.5}$ concentration of the BME model was on average lower than the actual data by 8.42% (95% CI: 0.05–34.52%)。

Secondly, for the backward trajectory model, air mass transport calculated by the HYSPLIT model strongly depends on the meteorological data set as input. Meteorological data errors imply inaccuracy of the trajectories. In our case, the Global Data Assimilation System (GDAS1) data originated from the National Centers for Environmental Prediction (NCEP) were applied as meteorological data to simulate transport trajectories. The GDAS is run 4 times a day (00, 06, 12, and 18 UTC) and the final output is for the analysis time and 3, 6, and 9-h forecasts (https://www.ready.noaa.gov/gdas1.php), with some variation from the observed data. Therefore, we compared the input data GDAS1 of the HYSPLIT model with the observed data. For wind speed, the difference between GDAS1 and monitoring data is on average 27.98% (95% CI: 0.11–39.45%); for wind direction, the difference is on average 24.26% (95% CI: 0.02–47.43%).

Finally, for the IER model, uncertainty primarily arises from challenges in accurately determining human exposure parameters and relies on simplified assumptions (Burnett et al. 2014). Meanwhile, variations between exposure concentrations and monitoring data at observation points also contribute to the overall uncertainty (Ping et al. 2023). However, due to limitations in manpower, financial resources, and technical capabilities, we currently lack the capacity to collect detailed exposure concentrations. Based on the limitations of $PM_{2.5}$ concentration estimation and meteorological data, the confidence interval of $PM_{2.5}$-related premature deaths was used to measure the uncertainty of the IER model (Fig. S7). The 4-year average number of deaths in Tianjin is 4310 deaths (95% CI: 2739; 5641) during 2017–2020.

In summary, the superposition of uncertainties from multiple data and parameters will affect the absolute value of the final calculation result, but the relative value impact is relatively small, that is, the ranking of premature deaths in each district remains unchanged. As a result, the BME-WCWT-IER models employed in this study are suitable for

calculating regional relative contributions of health burden, and the absolute values derived from the simulations are subject to inherent uncertainty.

Conclusions

In this paper, the BME-WCWT-IER method was developed to complete the quantitative traceability analysis of $PM_{2.5}$ pollution in the whole chain from emission-transport-health. Take Tianjin as an example, the results show that the potential transport direction within Tianjin was from south to north. Therefore, the districts distributed in the south of Tianjin are the focus areas on joint prevention and control. Furthermore, the industrial parks with high health burden are mainly distributed in the southern districts of Tianjin, which were consistent with the potential transport contribution results. In view of the above, it is necessary to focus on industrial parks in southern districts and take feasible and flexible measures according to different health burden levels. For example, it suggests that small industrial parks with high health burden can consider relocation policy. Based on the existing environment and abandoned facilities, relocated abandoned parks can be transformed into non-polluting parks, such as tourism parks with education and heritage, local culture, and tourism and recreation. Industrial tourism can help industrial operators create corporate value through service innovation.

This study has made three innovative attempts in the field of air pollution health research. First, previous studies have not integrated the health impacts of multiple industrial parks at the city level based on the BME-WCWT-IER model proposed in this article. This model provides $PM_{2.5}$ concentration data with a high spatial resolution (1 km), district-scale pollution transport, and $PM_{2.5}$-related premature deaths in industrial parks. Second, few studies have studied the health impacts of combining economic output. Third, few studies focused on Tianjin industrial parks. As a typical industrial city in China, the study of Tianjin can provide a mode to evaluate the health burden of industrial parks based on the $PM_{2.5}$ health impacts and industrial output, support formulation of joint prevention, and control policies and optimal layout of emission sources. In the future, the methodology proposed in this paper can be used to investigate a wider range of health burden related to air pollutants in other cities around the world with similar pollution emission characteristics and assess the health burden of their industrial parks lacking air pollution monitoring data. Based on the above considerations, fresh insights can be provided to them for city-level health management and environmental planning.

Supplementary Information The online version contains supplementary material available at https://doi.org/10.1007/s11356-023-29417-5.

Author contribution Mei Shan: conceptualization, data curation, visualization, project administration, writing draft. Yuan Wang: investigation, methodology, data curation. Zhi Qiao: conceptualization, investigation, methodology, formal analysis, validation. Yanwei Wang: investigation, methodology, validation, review and editing. Lien-Chieh Lee and Liying Ping: resources. Yun Sun: investigation, methodology, data curation. Zhou Pan: validation, resources, software.

Funding This work is financially supported by the National Natural Science Foundation of China (Grant No. 41871211).

Data availability The datasets used or analyzed during the current study are available from the corresponding author on reasonable request.

Declarations

Ethics approval This is a single study that does not split up into several parts to increase the quantity of submissions and is submitted to various journals or to one journal over time. Results are presented clearly, honestly, and without fabrication, falsification, or inappropriate data manipulation (including image-based manipulation). All authors have adhered to discipline-specific rules for acquiring, selecting, and processing data. No data, text, or theories by others are presented as if they were the author's own. And this study does not involve human subjects.

Consent to participate and for publication All authors have read and approved the paper and have agreed to participate and publish.

Competing interests The authors declare no competing interests.

References

Beckerman BS, Jerrett M, Serre M, Martin RV, Lee SJ, van Donkelaar A, Ross Z, Su J, Burnett RT (2013) A hybrid approach to estimating national scale spatiotemporal variability of $PM_{2.5}$ in the contiguous United States. Environ Sci Technol 47(13):7233–7241. https://doi.org/10.1021/es400039u

Burnett RT, Pope CA 3rd, Ezzati M, Olives C, Lim SS, Mehta S, Shin HH, Singh G, Hubbell B, Brauer M, Anderson HR, Smith KR, Balmes JR, Bruce NG, Kan H, Laden F, Prüss-Ustün A, Turner MC, Gapstur SM et al (2014) An integrated risk function for estimating the global burden of disease attributable to ambient fine particulate matter exposure. Environ Health Perspect 122(4):397–403. https://doi.org/10.1289/ehp.1307049

Cao J, Qiu X, Peng L, Gao J, Wang F, Yan X (2022) Impacts of the differences in $PM_{2.5}$ air quality improvement on regional transport and health risk in Beijing-Tianjin-Hebei region during 2013-2017. Chemosphere 297:134179. https://doi.org/10.1016/j.chemosphere.2022.134179

Chen L, Gao S, Zhang H, Sun Y, Ma Z, Vedal S, Mao J, Bai Z (2018) Spatiotemporal modeling of $PM_{2.5}$ concentrations at the national scale combining land use regression and Bayesian maximum entropy in China. Environ Int 116:300–307. https://doi.org/10.1016/j.envint.2018.03.047

Chen R, Li T, Huang C, Yu Y, Zhou L, Hu G, Yang F, Zhang L (2021) Characteristics and health risks of benzene series and halocarbons near a typical chemical industrial park. Environ. Pollut. (Barking, Essex: 1987). 289, 117893. https://doi.org/10.1016/j.envpol.2021.117893

Chen Y, Zhou Y, Zhao X (2020) $PM_{2.5}$ over North China based on MODIS AOD and effect of meteorological

elements during 2003–2015. Front. Environ. Sci. Eng. 10.1007/s11783-019-1202-8.
Christakos G (1990) A Bayesian maximum-entropy view to the spatial estimation problem. Math Geol 22(7):763–777. https://doi.org/10.1007/BF00890661
Cleland SE, West JJ, Jia Y, Reid S, Raffuse S, O'Neill S, Serre ML (2020) Estimating wildfire smoke concentrations during the October 2017 California fires through BME space/time data fusion of observed, Modeled, and Satellite-Derived $PM_{2.5}$. Environ Sci Technol 54(21):13439–13447. https://doi.org/10.1021/acs.est.0c03761
Ding D, Xing J, Wang S, Liu K, Hao J (2019) Estimated contributions of emissions controls, meteorological factors, population growth, and changes in baseline mortality to reductions in ambient PM2.5 and PM2.5-related mortality in China, 2013–2017. Environ Health Perspect 127(6):067009. https://doi.org/10.1289/EHP4157
Hao TY, Cai Z, Chen S, Han S (2019) Transport pathways and potential source regions of $PM_{2.5}$ on the West Coast of Bohai Bay during 2009-2018. Atmosphere. 10(6):345. https://doi.org/10.3390/atmos10060345
Han X, Sun T, Feng Q (2019a) Study on environmental pollution loss measurement model of energy consumption emits and its application in industrial parks. Sci Total Environ 668:1259–1266. https://doi.org/10.1016/j.scitotenv.2019.03.002
Han S, Cai Z, Liu J, Zhang M, Chen J, Lin Y (2019b) Comparison on aerosol physicochemical properties of sea and land along the coast of Bohai, China. Sci Total Environ 673:148–156. https://doi.org/10.1016/j.scitotenv.2019.04.040
He G, Pan Y, Tanaka T (2020) The short-term impacts of COVID-19 lockdown on urban air pollution in China. Nat. Sustain. 1-7. https://doi.org/10.1038/s41893-020-0581-y
Huang, Y., Unger, N., Harper, K., Heyes, C., (2020a (a)). Global climate and human health effects of the gasoline and diesel vehicle fleets. GeoHealth 4 (3). https://doi.org/10.1029/2019GH000240.
Huang X, Ding A, Wang Z, Ding K, Gao J, Chai F, Fu C (2020b) Amplified transboundary transport of haze by aerosol–boundary layer interaction in China. Nat Geosci 13:428–434. https://doi.org/10.1038/s41561-020-0583-4
Huang C, Hu J, Xue T, Xu H, Wang M (2021) High-resolution spatiotemporal modeling for ambient $PM_{2.5}$ exposure assessment in China from 2013 to 2019. Environ Sci Technol 55(3):2152–2162. https://doi.org/10.1021/acs.est.0c05815
Jiang Y, Xing J, Wang S, Chang X, Liu S, Shi A et al (2021) Understand the local and regional contributions on air pollution from the view of human health impacts. Front Environ Sci 15(5):1–11. https://doi.org/10.1007/s11783-020-1382-2
Li Y, Li B, Liao H, Zhou B, Wei J, Wang Y, Zang Y, Yang Y, Liu R, Wang X (2022) Changes in $PM_{2.5}$-related health burden in China's poverty and non-poverty areas during 2000-2020: a health inequality perspective. Sci Total Environ. 160517 https://doi.org/10.1016/j.scitotenv.2022.160517
Lin H, Taniyasu S, Yamashita N, Khan MK, Masood SS, Saied S, Khwaja HA (2022) Per- and polyfluoroalkyl substances in the atmospheric total suspended particles in Karachi, Pakistan: profiles, potential sources, and daily intake estimates. Chemosphere. 288:132432. https://doi.org/10.1016/j.chemosphere.2021.132432
Lee CJ, Martin RV, Henze DK, Brauer M, Cohen A, Donkelaar AV (2015) Response of global particulate-matter-related mortality to changes in local precursor emissions. Environ Sci Technol 49(7):4335–4344. https://doi.org/10.1021/acs.est.5b00873
Lyu Y, Liu Y, Guo Y, Sang J, Tian J, Chen L (2022) Review of green development of Chinese industrial parks. Energy Strat Rev 42:100867. https://doi.org/10.1016/j.esr.2022.100867
Ping L, Wang Y, Lu Y, Lee LC, Liang C (2023) Tracing the sources of $PM_{2.5}$-related health burden in China. Environ. Pollut. (Barking, Essex: 1987), 327, 121544. https://doi.org/10.1016/j.envpol.2023.121544
Randles CA, Da Silva AM, Buchard V, Colarco PR, Darmenov A, Govindaraju R, Smirnov A, Holben B, Ferrare R, Hair J, Shinozuka Y, Flynn CJ (2017) The MERRA-2 aerosol reanalysis, 1980 - onward, part I: system description and data assimilation evaluation. J Clim 30(17):6823–6850. https://doi.org/10.1175/JCLI-D-16-0609.1
Reyes JM, Serre ML (2014) An LUR/BME framework to estimate $PM_{2.5}$ explained by on road mobile and stationary sources. Environ Sci Technol 48(3):1736–1744. https://doi.org/10.1021/es4040528
Shan M, Liang S, Fu H, Li X, Teng Y, Zhao JW, Liu YX, Cui C, Chen L, Yu H, Yu SB, Sun YL, Mao J, Zhang H, Gao S, Ma ZX (2021) Spatial prediction of soil calcium carbonate content based on Bayesian maximum entropy using environmental variables. Nutr Cycl Agroecosyst 120(1):17–30. https://doi.org/10.1007/s10705-021-10135-8
Song Z, Fu D, Zhang X, Wu Y, Xia X, He J, Han X, Zhang R, Che H (2018) Diurnal and seasonal variability of $PM_{2.5}$ and AOD in North China plain: comparison of MERRA-2 products and ground measurements. Atmos Environ 191:70–78. https://doi.org/10.1016/J.ATMOSENV.2018.08.012
Sun S, Zheng N, Wang S, Li Y, Hou S, Song X, Du S, An Q, Li P, Li X, Hua X, Dong D (2021) Source analysis and human health risk assessment based on entropy weight method modification of $PM_{2.5}$ heavy metal in an industrial area in the northeast of China. Atmos. 12:852. https://doi.org/10.3390/atmos12070852
Tang X, Chen X, Tian Y (2017) Chemical composition and source apportionment of $PM_{2.5}$ – a case study from one year continuous sampling in the Chang-Zhu-Tan urban agglomeration. Atmos Pollut Res 8:885–899. https://doi.org/10.1016/J.APR.2017.02.004
Tianjin Statistical yearbook 2018-2021. https://stats.tj.gov.cn/nianjian/2021nj/zk/indexch.htm (accessed 13 March 2022)
Wang YQ, Zhang XY, Arimoto R (2006) The contribution from distant dust sources to the atmospheric particulate matter loadings at Xian, China during spring. Sci Total Environ 368:875–883. https://doi.org/10.1016/j.scitotenv.2006.03.040
Wang YQ, Zhang XY, Draxler RR (2009) TrajStat: GIS-based software that uses various trajectory statistical analysis methods to identify potential sources from long-term air pollution measurement data. Environ Model Softw 24:938–939. https://doi.org/10.1016/j.envsoft.2009.01.004
Wang Y, Ge X, Liu J, Ding Z (2016) Study and analysis of energy consumption and energy-related carbon emission of industrial in Tianjin, China. Energy Strat Rev 10:18–28. https://doi.org/10.1016/J.ESR.2016.04.002
Wang Y, Wang Y, Zhang Z, Zhang L, Shan M (2022) Analysis of potential source areas and transport pathways of $PM_{2.5}$ and O_3 in Tianjin by season. Res Environ Sci 35(03):673–682. https://doi.org/10.13198/j.issn (Chinese)
Wang J, Bradbury JH (1986) The changing industrial geography of the Chinese special economic zones. Econ Geogr 62:307–320. https://doi.org/10.2307/143827
Wu R, Bo Y, Li J, Li L, Li Y, Xie S (2016) Method to establish the emission inventory of anthropogenic volatile organic compounds in China and its application in the period 2008–2012. Atmos Environ 127:244–254. https://doi.org/10.1016/j.atmosenv.2015.12.015
Wu S, Wang Y, Canwen C, Cao Z, Jiaxuan C, Yu Z, Song H (2021) Valley city ventilation under the calm and stable weather conditions: a review. Build Environ 194:107668. https://doi.org/10.1016/J.BUILDENV.2021.107668
Xiao L, Lang Y, Christakos G (2018) High-resolution spatiotemporal mapping of $PM_{2.5}$ concentrations at Mainland China using a combined BME-GWR technique. Atmos Environ 173:295–305. https://doi.org/10.1016/J.ATMOSENV.2017.10.062
Xiong H, Chen J, Ma X, Fang M (2021) Estimating the $PM_{2.5}$ concentration over Anhui Province, China, using the Himawari-8 AOD

and a GAM/BME model. Atmos Pollut Res 12:101–110. https://doi.org/10.1016/j.apr.2021.101110

Xu F, Xiang N, Tian J, Chen L (2017a) 3Es-based optimization simulation approach to support the development of an eco-industrial park with planning towards sustainability: a case study in Wuhu, China. J Clean Prod 164:476–484. https://doi.org/10.1016/J.JCLEPRO.2017.06.192

Xu Y, Serre ML, Reyes JM, Vizuete W (2017b) Impact of temporal upscaling and chemical transport model horizontal resolution on reducing ozone exposure misclassification. Atmos Environ 166:374–382. https://doi.org/10.1016/J.ATMOSENV.2017.07.033

Xu T, Zhang C, Liu C, Hu Q (2023) Variability of $PM_{2.5}$ and O_3 concentrations and their driving forces over Chinese megacities during 2018-2020. J Environ Sci (China) 124:1–10. https://doi.org/10.1016/j.jes.2021.10.014

Zhang C, Zhang Y, Liu X, Liu Y, Li C (2023) Characteristics and source apportionment of $PM_{2.5}$ under the dual influence of the Spring Festival and the COVID-19 pandemic in Yuncheng city. J Environ Sci (China) 125:553–567. https://doi.org/10.1016/j.jes.2022.02.020

Zhang RJ, Jing J, Tao J, Hsu SC, Wang G, Cao J, Lee CSL, Zhu L, Chen Z, Zhao Y, Shen Z (2013) Chemical characterization and source apportionment of $PM_{2.5}$ in Beijing: seasonal perspective. Atmos Chem Phys 13:7053–7074. https://doi.org/10.5194/ACP-13-7053-2013

Zhang X, Wang H, Li Y, Lan L, Zhang J, Li X, Jia Z (2021) Identification of the health risk zones of nitrogen oxides in typical industry develop planning. Air Qual Atmos Health 14:1393–1404. https://doi.org/10.1007/s11869-021-01029-3

Zheng H, Kong S, Yan Y, Chen N, Yao L, Liu X, Wu F, Cheng Y, Niu Z, Zheng S, Zeng X, Yan Q, Wu J, Zheng M, Liu D, Zhao D, Qi S (2020) Compositions, sources and health risks of ambient volatile organic compounds (VOCs) at a petrochemical industrial park along the Yangtze River. Sci Total Environ 703:135505. https://doi.org/10.1016/j.scitotenv.2019.135505

This paper has not been published previously, and it is not being considered by any other peer-reviewed journal. The submitted work is original and does not have been published elsewhere in any form or language.